Measurement of Positron Range in Matter in Strong Magnetic Fields

Bruce E. Hammer[1] and Nelson L. Christensen[2]

[1]University of Minnesota, Department of Radiology, Minneapolis, MN 55455 U.S.A.
[2]University of Auckland, Department of Physics, Auckland, NZ

Abstract

Positron range is one factor that places a limitation on Positron Emission Tomography (PET) resolution. The distance a positron travels through matter before it annihilates with an electron is a function of its initial energy and the electron density of the medium. A strong magnetic field limits positron range when momentum components are transverse to the field. Measurement of positron range was determined by deconvolving the effects of detector response and radioactivity distribution from the measured annihilation spread function. The annihilation spread function for a 0.5 mm bead of ^{68}Ga was measured with 0.2 and 1.0 mm wide slit collimators. Based on the annihilation spread function FWHM (Full Width at Half Maximum) for a 1.0 mm wide slit the median positron range in tissue equivalent material is 0.87, 0.50, 0.22 mm at 0, 5.0 and 9.4 T, respectively.

I. INTRODUCTION

Positron annihilation in a magnetic field leads to a quenching of positronium decay [1] and a decrease in positron range [2,3]. It is the magnetic field's effect on positron range that has practical consequences for PET imaging and radiotherapy applications [4]. For the case of PET, positron annihilation can be detected in strong magnetic fields with magnetically field tolerant photodiodes [3] or lightguides coupled to a PMT located in a low magnetic field [5,6]. This manuscript describes the quantitative measurement of positron range in tissue equivalent material in a magnetic field.

The authors gratefully acknowledge Intermagnetics General Corporation, Latham, NY for loaning the nuclear instrumentation. Dr.'s K. Ugurbil, M. Garwood and H. Merkle for 9.4 T magnet access at the Center for Magnetic Resonance Research, University of MN, Minneapolis, MN. Supported by U.S. Public Service Grant (1 R03 RR07042-01).

There are two driving forces for acquiring a PET image in a strong magnetic field. The first is to reduce image blur from positron range effects for images transverse to the magnetic field, Figure 1. The second is to obtain simultaneous PET and MR (Magnetic Resonance) images within the same scanning apparatus. Operating a PET or hybrid MR-PET scanner in a magnetic field requires significant engineering modifications and data acquisition challenges. Addressing the details of these engineering issues are beyond the scope of this paper.

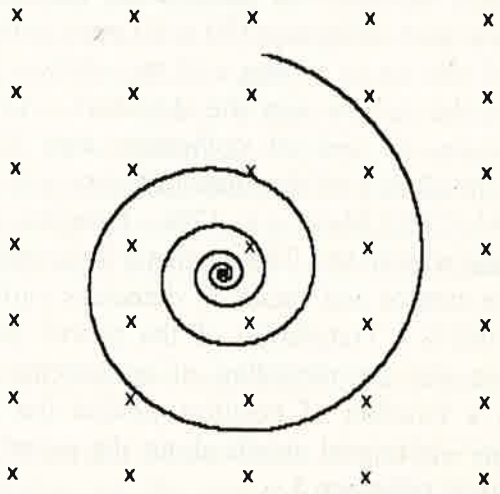

Figure 1: Idealized trajectory of positron in a magnetic field when moving transverse, i.e. perpendicular, to an external magnetic field. The positron spirals because of energy loss due to ionizations and excitations with atoms in matter. The magnetic field has no effect when positron velocity is longitudinal, i.e. parallel, to the magnetic field.

II. METHODS

Measuring the variation of point spread or line spread function as a function of positron energy and density of medium yields an estimate of positron range in matter [7,8]. Translating a positron source past a pair of opposed lead-collimated scintillation

0018-9499/95$4.00

detectors and recording coincident events, as a function of position, in a window centered around 0.511 MeV results in a curve that approximates a Gaussian function in a magnetic field or a biexponential function with long tails at zero field.

A 0.5 mm diameter resin bead impregnated with 100 mCi of ^{68}Ga (Isotope Products Laboratories, Berkeley, CA) was placed in the center of a 2.5 cm x 2.5 cm cylinder of tissue equivalent wax (Radiation Products Design, Inc., Albertsville, MN). The mean and maximum energy of ^{68}Ga positrons are 0.81 and 1.9 MeV, respectively [9]. The radioactive sample was mounted to a non-magnetic movable platform (Velmex, East Bloomfield NY) and placed in the center of either a 5.0 T/0.4 m or 9.4 T/0.3 m (Magnex Scientific LTD., Abingdon, England) magnet. A pair of opposing 28x28x28 mm CsI scintillators mounted to 18x18 mm photodiode (EV Products, Saxon, PA) detectors operating at +42V bias detected the annihilation photons. A cylindrical lead collimator (50 x 50 mm) with a 0.2 mm x 25 mm slit or a 1mm x 25 mm slit was placed between the sample and the detectors. Distance from source to end of collimator was 82 mm. Energy resolution of the discriminators was set at 0.511 +/- 0.032 MeV, e.g. 13%. Detector energy resolution was 10 %. The magnetic field uniformity over the sample and radiation detectors varies less than 0.001%. Translation of the source past the detectors and the recording of coincidence count rate as a function of position yielded the spread function. Additional details about the experimental setup are in reference 3.

III. RESULTS

Effect of Collimator on FWHM Measurement

A 5 cm thick lead collimator was placed in front of each 25 x 25 mm CsI(Tl) crystal used for coincidence detection of annihilation photons. One set of collimators (two per set) had a 1 x 25 mm slit while the other collimator set had a 0.2 x 25 mm slit. Coincidence measurements were made with either a pair of 0.2 mm slits or a pair of 1.0 mm slits. Table I shows the effect of slit width on the measured FWHM and FWTM (Full Width at Tenth Maximum). The smaller slit yields a narrower FWHM and thus a more accurate measurement of positron range. Table II shows the difference in FWHM and FWTM when comparing the spread functions from 0.2 mm and 1.0 mm slits.

Table I: Measurement of spread function FWHM and FWTM as a function of collimator slit width. Measurement error is less than 5%.

	0.2 mm slit		1.0 mm slit	
Field (T)	FWHM (mm)	FWTM (mm)	FWHM (mm)	FWTM (mm)
0.0	2.00	6.50	2.30	7.10
5.0	1.40	3.00	1.62	3.42
9.4	0.93	1.88	1.12	2.27

Table II: Difference in FWHM and FWTM when measuring annihilation spread function with 0.2 mm and 1.0 mm slit widths. Breadth of the annihilation function decreases for the smaller slit width.

Field (T)	Δ FWHM (mm)	Δ FWTM (mm)
0.0	0.30	0.60
5.0	0.22	0.42
9.4	0.19	0.39

Effect of Bead's Radioisotope Distribution on FWHM Measurement

The ideal method to measure positron range is to have an infinitesimally small high specific activity positron source inside of a homogenous medium. The smallest dimension source we could obtain was a 0.5 mm cation exchange resin bead impregnated with ^{68}Ga (Isotope Products Laboratories, Berkeley, CA). Close inspection of the annihilation spread functions, at all fields, yields a slight asymmetry of the curve. This is probably due to a nonuniform distribution of radioisotope on the bead. The most likely distribution of or radioactivity is a gradient from one side of the bead to the other. Bead radioisotope distribution was simulated on a computer as either a uniform distribution or a shell of radioisotope that penetrated 20% beyond the bead's surface.

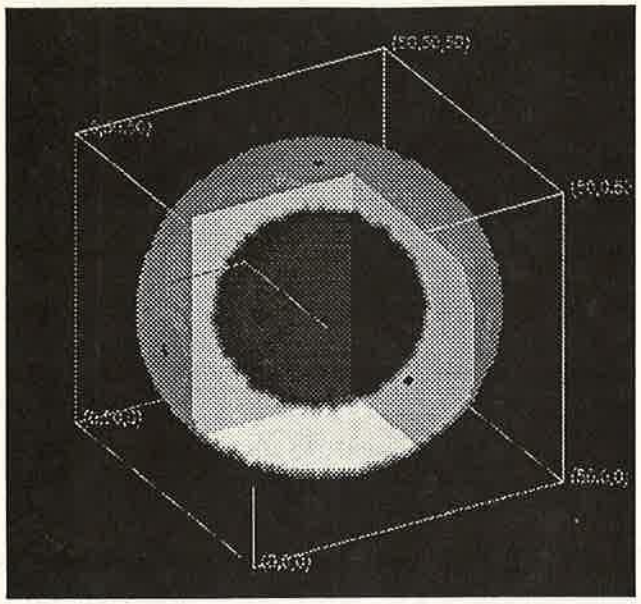

Figure 2a

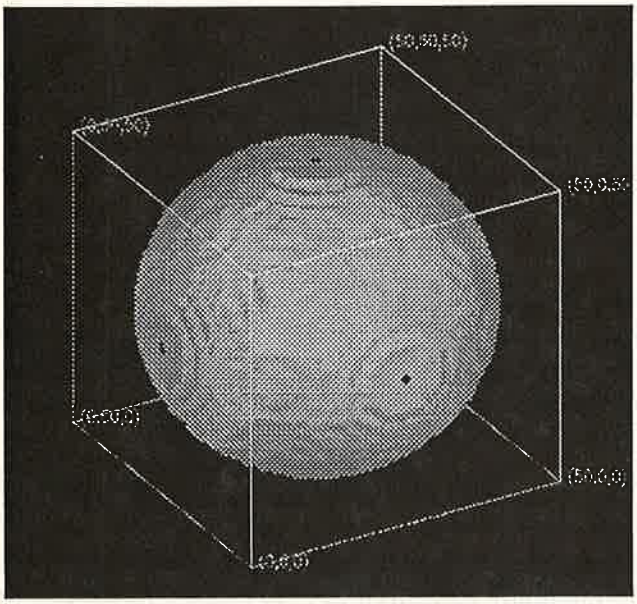

Figure 2b

Figure 2: (a) Simulation of a 0.5 mm diameter bead with a 0.1 mm shell of radioisotope; (b) simulation of same bead with uniform radioisotope distribution throughout its volume.

Figure 2a shows a cut through a bead that has a radioisotope penetrating 0.1 mm into a 0.5 mm ion exchange resin. Figure 2b shows a uniform density of radioisotope throughout the bead. Both of these radioisotope distributions are consistent with the physical chemical properties of ion exchange resins.

IV. DISCUSSION

Measuring the variation of point spread or line spread function as a function of positron energy and density of medium yields an estimate of positron range in matter [7,10]. Translating a positron source past a pair of opposed lead-collimated scintillation detectors and recording coincident events, as a function of position, in a 0.511 ± 0.032 MeV energy window results in a curve that approximates a Gaussian function. A common definition of positron range is based on measuring the FWHM or FWTM of a spread function. The measured spread function is a convolution of detector aperture, positron range, and source dimension; the positron range is therefore complicated to determine.

Positrons are emitted isotropically; the radial distribution of annihilation events is a convolution of an isotope's positron energy spectrum with the distribution of radial distance a specific energy positron travels before annihilation. Imposition of a strong magnetic field decreases the radial distance of positron travel transverse to the field [2,3] whereas positron range longitudinal to the field is unaffected [3].

Effect of Collimator on FWHM Measurement

Experimental measurement of positron range is a convolution of the energy spectrum with radial distance a positron travels before meeting and annihilating with an electron. The measured spread function is a convolution of detector aperture, positron range, and source dimension that complicates the absolute determination of positron range in matter.

The FWHM depends on detector aperture, angular deviation of annihilation photons and effective source size [11]:

$$\Gamma = \sqrt{(d/2)^2 + (0.0022D)^2 + s^2} \qquad (1)$$

where d is the collimator width, D is the separation between the crystal pair and s is the effective source size. The 0.0022 factor is from the angular deviation of annihilation photons, which is approximately Gaussian and has a FWHM of 8.7 mrad [12,13]. The effective source size consists of the physical dimensions of the radioactive source and the positron range before annihilation. The term 0.0022 is no longer a constant when the solid angle of a collimator is less than 8.7 mrad. Thus equation (1) becomes:

$$\Gamma = \sqrt{(d/2)^2 + (\Omega D)^2 + (2(r+R))^2} \qquad (2)$$

where r is the radius of the radioactive bead, R is the range the positron travels before annihilation, Ω is the solid angle of the collimator when $\Omega < 8.7$ mrad. For the 0.2 mm slit Ω is 2.4 mrad. As $R \rightarrow 0$ equation (2) approaches equation (1) when $\Omega > 8.7$ mrad..

To examine the effect of collimator slit width on the annihilation distribution function the slit width was convoluted with the bead's radioisotope distribution and simulated on a personal computer. The bead's 3-D radioactive distribution was assumed to be either a spherical shell or a uniformly labeled sphere (Fig. 2). The bead's radioisotope distribution was modeled as a 1-D projection through an equatorial slice (Fig. 3). This is what we actually measure through a collimator slit in an experiment.

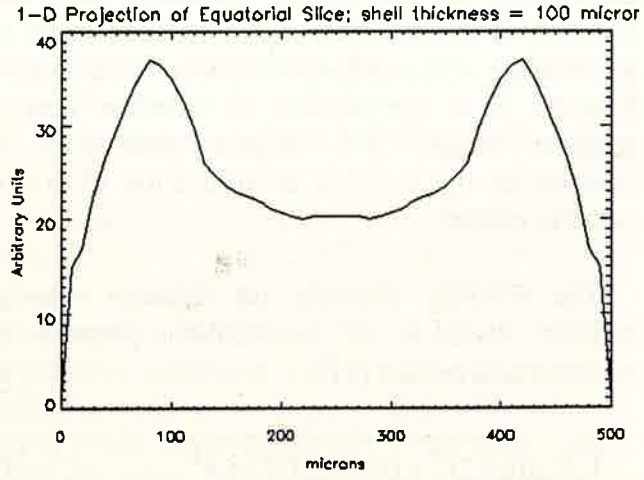

Figure 3a

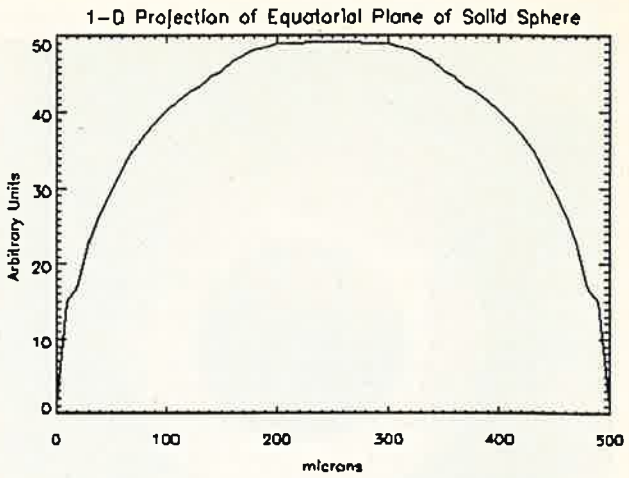

Figure 3b

Figure 3: Simulation of radioisotope projection through equatorial plane of a 0.5 mm diameter resin bead with (a) 0.1 mm shell of radioisotope; (b) solid sphere of radioisotope.

The 1-D projection of radioactivity was convoluted with slit widths of 2.0, 1.0, 0.2 and 0.0 mm using equation (3).

$$f(x) = e(x) \otimes h(x) = \int_{-\infty}^{+\infty} e(x')h(x-x')dt \qquad (3)$$

where e(x) is the distribution of bead radioactivity, h(x) is the slit width. The actual limits of integration in the simulation are 100 x the slit width. The results of these simulations are shown in Figure 4.

Using a 0.2 mm slit resolves the 0.1 mm shell of radioisotope on the 0.5 mm diameter bead. These simulations imply that analyzing the shape of the experimentally measured spread function can lead to insight if the bead's radioactive distribution is uniform or a shell. The measured spread function displayed no evidence of a bimodal distribution function for measurements with the 0.2 mm slit. This may imply that the radioisotope distribution penetrated throughout the bead. Note that these simulations do not include positron range effects. Convoluting positron range effects with these data tend to blur out the radioactivity distribution that is seen for small slit widths.

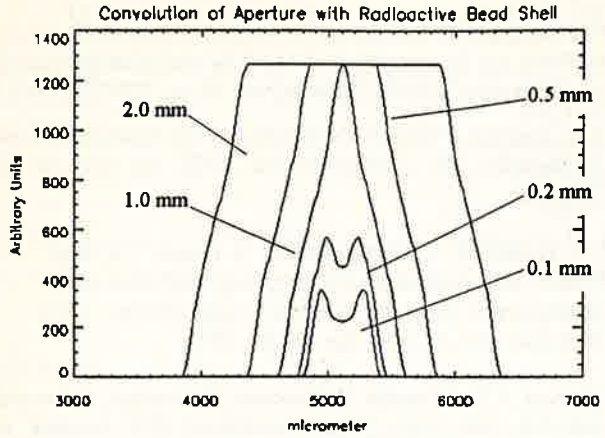

Figure 4a

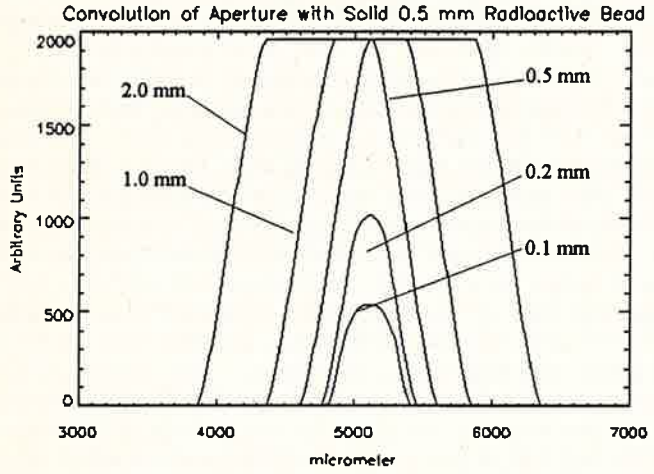

Figure 4b

Figure 4: Convolution of 0.1, 0.2, 0.5, 1.0, 2.0 mm collimator slits with radioisotope projections of Fig. 3. Note increase in counts and loss of spatial resolution at larger slit widths.

Figure 5 is a plot of equation (2) where the theoretical FWHM is a function of slit widths and a continuum of positron ranges. Note that using a 0.2 mm slit width has a minimal effect on the measured FWHM. Table II shows the change in FWHM between using a 1.0 mm and 0.2 mm slit. The difference in FWHM predicted by equation 2 and Figure 5 agrees well with the 5.0 T and 9.4 T data. A discrepancy exists for the 0 T data that is probably due to the biexponential behavior of the spread function [14].

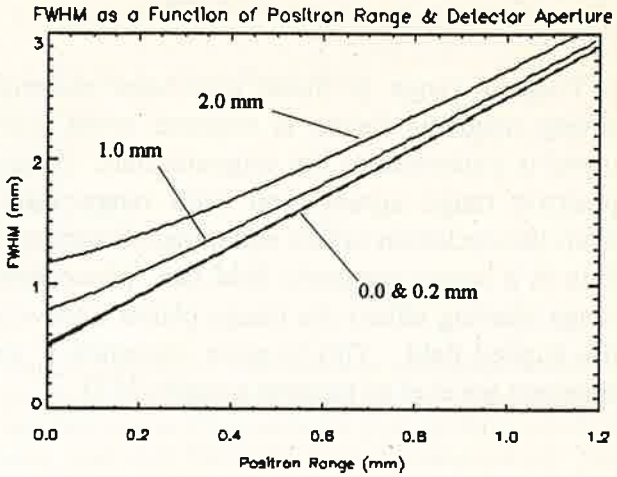

Figure 5: Physical diameter of source = 0.5 mm; crystal to crystal distance = 164 mm, slit = 2.0 mm; 1.0 mm, 0.2 mm, 0 mm. Plots based on eqn. (2).

The positron range calculated from the cyclotron radius is very close to the experimentally measured range. In vacuum, a positron with momentum P (MeV/c), moving transverse to the magnetic field B (T), moves in a circular orbit with a radius described by

$$R_c = \frac{P}{2.998 * B} \qquad (4)$$

Twice the cyclotron radius (R_c) for the average positron energy plus the bead diameter gives an estimate for positron range in a magnetic field, i.e, FWHM = $2R_c$ + bead diameter. Assuming a median positron energy of 0.81 MeV [9] and equation (4) the cyclotron radius of a positron, in vacuum, calculates to be very close to the experimental measurement (Table III). This is both satisfying and surprising because of the tortuous path an electron takes through matter as a result of elastic and inelastic collisions.

Table III: Comparison of positron range calculated from FWHM of 0.2 mm slit and 1.0 mm slit (in parenthesis) with cyclotron radius i.e., equation (4).

Field (T)	Positron Range from FWHM (mm)	Positron Range from Cyclotron Radius (mm)
5.0	0.45 (0.50)	0.54
9.4	0.22 (0.22)	0.29

V. CONCLUSION

Positron range in tissue equivalent material, in strong magnetic fields, is reduced when positron travel is transverse to the magnetic field. Measured positron range agrees well with range estimates from the cyclotron radius equation. Acquiring PET data in a strong magnetic field can reduce positron range blurring effects for image planes transverse to the applied field. This is quite important if animal scanners are ever to become a reality [15].

VI. REFERENCES

[1] O. Halpern,"Magnetic Quenching of Positronium Decay," Phys. Rev., vol. 94, No. 4, pp. 904 - 907, 1954.

[2] H. Iida, I. Kanno, S. Miura, M. Murakami, K. Takahashi and K. Uemura, "A Simulation Study of a Method to Reduce Positron Annihilation Spread Distributions Using a Strong Magnetic Field in Positron Emission Tomography", IEEE Trans. Nucl. Sci., vol. 33, pp. 597-600, 1986.

[3] B.E. Hammer, N.L. Christensen and B.G. Heil, "Use of a Magnetic Field to Increase the Spatial Resolution of Positron Emission Tomography", Medical Physics, vol. 21, no. 11, pp. 1917 - 1920, 1994.

[4] R.R. Raylman, R.L. Wahl, "Magnetically Enhanced Radionuclide Therapy," J. Nucl. Med., vol. 305, no. 1, pp. 157-163, 1994.

[5] N.L. Christensen, B.E. Hammer, B.G. Heil, K. Fetterly, "A Technique for Positron Emission Tomography Use in Magnetic Fields with Photomultipliers and Lightguides," Phys. Med. Biol., accepted for publication, 1995.

[6] Hammer, "NMR-PET Scanner Apparatus," U.S.Patent Number 4,939,464: July 3, 1990.

[7] Z.H. Cho, J.K. Chan, L. Ericksson, M. Singh, S. Graham, N.S. MacDonald, Y. Yano, "Positron Ranges Obtained from Biomedically Important Positron-Emitting Radionuclides,",J. Nucl. Med., vol. 16, pp. 1174-1176, 1975.

[8] M.E. Phelps, E.J. Hoffman, S-C Huang and M.M. Ter-Pogossian, "Effect of Positron Range on Spatial Resolution", J. Nucl. Med., vol. 16, **pp.** 649-652, 1975.

[9] Hogan, O.L., Beta Spectra V. Spectra of Individual Positron Emitters, USNRDL-TR-1101, 14 November 1966.

[10] S.E. Derenzo, "Precision Measurement of Annihilation Point Spread Distributions for Medically Important Positron Emitters," Proc. 5th Int. Conf. Positron Annihil., Lake Yamanaka, Japan, pp. 819-823, 1979.

[11] W.W. Moses, S.E, Derenzo, "Empirical Observation of Resolution Degredation in Positron Emission Tomographs Utilizing Block Detectors," J. Nucl Med, vol. 34:5, 101P, 1993.

[12] P. Colombino, B. Fiscella and L. Trossi, "Study of Positronium in Water and Ice from 22 to -144 °C by Annihialtion Quantum Measurements," Nuovo Cimento, vol. 38, pp. 707-723, 1965.

[13] S.E. Derenzo, "Recent Developments in Positron emission Tomography (PET) Instrumentation, SPIE, vol. 671, pp. 232-243, 1986.

[14] C.J. Thompson, J. Moreno-Cantu, Y. Picard, "PETSIM: Monte Carlo simulation of all sensitivity and resolution parameters of cylindrical positron imagingsystems," Phys. Med. Biol., vol.37, no.3, pp. 731-49, 1992.

[15] Marriott, J.E. Cadorette, R. Lecomte, V. Scasnar, J. Rousseau and J.E. van Lier, "High Resolution PET Imaging and Quantitation of Pharmaceutical Biodistributions in Small Animal Using Avalanche Photodiode Detectors," J. Nucl. Med., vol. 35, pp. 1390-1396 1994.